HHS Public Access

Author manuscript

Biomaterials. Author manuscript; available in PMC 2019 July 01.

Published in final edited form as:

Biomaterials. 2018 July ; 172: 54–65. doi:10.1016/j.biomaterials.2018.04.047.

Design of a vascularized synthetic poly(ethylene glycol) macroencapsulation device for islet transplantation

Jessica D. Weaver[a], **Devon M. Headen**[a], **Michael D. Hunckler**[a], **Maria M. Coronel**[a], **Cherie L. Stabler**[b], and **Andrés J. García**[a,†]

[a]Woodruff School of Mechanical Engineering and Petit Institute for Bioengineering and Bioscience, Georgia Institute of Technology, Atlanta, GA 30332, USA

[b]Department of Biomedical Engineering, University of Florida, Gainesville, FL 32611, USA

Abstract

The use of immunoisolating macrodevices in islet transplantation confers the benefit of safety and translatability by containing transplanted cells within a single retrievable device. To date, there has been limited development and characterization of synthetic poly(ethylene glycol) (PEG)-based hydrogel macrodevices for islet encapsulation and transplantation. Herein, we describe a two-component synthetic PEG hydrogel macrodevice system, designed for islet delivery to an extrahepatic islet transplant site, consisting of a hydrogel core cross-linked with a non-degradable PEG dithiol and a vasculogenic outer layer cross-linked with a proteolytically sensitive peptide to promote degradation and enhance localized vascularization. Synthetic PEG macrodevices exhibited equivalent passive molecular transport to traditional microencapsulation materials (e.g., alginate) and long-term stability in the presence of proteases *in vitro* and *in vivo,* out to 14 weeks in rats. Encapsulated islets demonstrated high viability within the device *in vitro* and the incorporation of RGD adhesive peptides within the islet encapsulating PEG hydrogel improved insulin responsiveness to a glucose challenge. *In vivo*, the implementation of a vasculogenic, degradable hydrogel layer at the outer interface of the macrodevice enhanced vascular density within the rat omentum transplant site, resulting in improved encapsulated islet viability in a syngeneic diabetic rat model. These results highlight the benefits of the facile PEG platform to provide controlled presentation of islet-supportive ligands, as well as degradable interfaces for the promotion of engraftment and overall graft efficacy.

†Corresponding author: andres.garcia@me.gatech.edu.

7. Data availability

The datasets generated during and/or analyzed during the current study are available from the corresponding author on reasonable request.

6. Competing interests

The authors confirm that there are no known conflicts of interest associated with this publication and there has been no significant financial support for this work that could have influenced its outcome.

Keywords

islet transplantation; vascularization; encapsulation; omentum transplantation

1. Introduction

Type 1 diabetes (T1D) mellitus, characterized by the autoimmune destruction of insulin-secreting beta cells within pancreatic islets, affects 1.25 million individuals in the United States [1], resulting in a $15 billion annual financial burden [2]. Current treatment for T1D is limited to exogenous insulin injections, which cannot adequately restore normal glycemic control, resulting in a high incidence of long term secondary complications [3]. Islet cell replacement therapy has demonstrated the ability to restore native insulin signaling patterns and has the potential to eliminate long term complications of the disease [4, 5]. The required chronic systemic immunosuppression regimen for this allogeneic organ transplant, however, is an unrealistic burden for the vast majority of T1D patients [6], necessitating alternative strategies to mitigate immune rejection of transplanted islets that can widen the applicability of this transformative therapy for insulin-dependent patient populations [7].

Encapsulation of transplanted cells within biomaterials has long been proposed as a method of circumventing chronic systemic immunosuppression by preventing the cell-to-cell contact that results in direct antigen recognition by the immune system [8–10]. This strategy spans the scale of nano-, micro-, and macro-encapsulation [11, 12]. Microencapsulation is the most heavily investigated strategy, wherein 1–3 islets are commonly encapsulated within a hydrogel and delivered to the intraperitoneal space [9], due to the space required by the volume of such a graft [13]. To date, there has been limited translational success of microencapsulation due to lack of graft function, as well as safety limitations of non-retrievable capsules within the intraperitoneal space. Human trials demonstrate microcapsule adhesion to parietal peritoneum, spleen, kidney, and omentum, raising concerns about the long-term safety of intraperitoneal capsule delivery [14].

Macrodevices for islet encapsulation have been explored in preclinical and clinical trials [14–18] and confer the safety benefit of a single, retrievable device. As islets exhibit elevated oxygen consumption rates compared to other cell types [19, 20], the primary limitation of these devices is adequate oxygenation of the encapsulated islets. Strategies to address this limitation include oxygen-perfused devices that require daily replenishment [6], prevascularized devices [16, 21, 22], oxygen-generating devices [23], scaffold-type devices for optimal islet spacing [24], and/or the infusion of soluble vasculogenic factors to stimulate greater vascularization at the device surface [25]. Whereas vascularization strategies demonstrate improvements in islet survival, these devices have typically been implemented in the subcutaneous space, which demonstrates relatively poor capacity for vascular enhancement, as well as glycemic control [26]. As such, it is critical that islet macroencapsulation devices are designed for adequate oxygen distribution, with strategies that maximize vascularization at the device surface.

We have shown that controlled vasculogenic endothelial growth factor (VEGF) delivery via a synthetic, degradable hydrogel matrix enhances functional vascularization within

extrahepatic islet transplant sites [26–28], improving islet viability and function. This prior work focused on fully degradable materials that were replaced by tissue within a few weeks. Herein, we sought to translate this validated vasculogenic platform to improve the engraftment of a synthetic, poly(ethylene glycol) (PEG)-based nondegradable hydrogel macrodevice designed to encapsulate islets for isolated and retrievable delivery to a transplantation site (Fig. 1). Increasing the vascular density at the interface of an immunisolating macrodevice should improve both nutritional delivery to encapsulated islets and insulin responsiveness, thereby enhancing overall graft durability and efficacy.

2. Materials and Methods

2.1. Materials

Chemicals were obtained from Sigma Aldrich (St. Louis, MO) and cell culture materials were obtained from Thermo Fisher (Carlsbad, CA), unless otherwise noted. Peptides were obtained from Genscript (Piscataway, NJ) unless otherwise noted.

2.2. Macrodevice fabrication and characterization

2.2.1. Gel fabrication—Four-arm maleimide-end functionalized PEG macromer (PEG-MAL 20 kDa, >95% functionalization, Laysan Bio, Arab, AL) was functionalized with recombinant human VEGF-A165 (Invitrogen, Carlsbad, CA) for 15 min in 25 mM HEPES buffer (DPBS with calcium and magnesium) at pH 7.4 followed by functionalization with either RGD peptide (GRGDSPC) or RDG scrambled peptide (GRDGSPC). Functionalized macromers were cross-linked using either the bi-cysteine peptides VPM (GCRDVPMSMRGGDRCG) or GDQ (GCRDGDQGIAGFDRCG) (Aapptec, Louisville, KY), or PEG-dithiol (314 Da). Gels crosslinked with VPM, GDQ, and PEGDT are designated as PEG/VPM, PEG/GDQ, and PEG/PEGDT, respectively. The PEG-MAL hydrogels were synthesized at the indicated weight percentages (5.0 or 7.0% wt/vol.) to obtain a final concentration of 1.0 mM adhesive peptide and 10 μg/mL VEGF unless otherwise noted. The concentration of cross-linker used for the synthesis of each hydrogel was calculated by matching the number of cysteine residues on the cross-linker to the number of residual maleimides on the PEG-MAL macromer following adhesive peptide and VEGF functionalization.

2.2.2. Rheology measurements—The storage and loss moduli of hydrogels were assessed by dynamic oscillatory strain and frequency sweeps performed on a MCR 302 stress-controlled rheometer (Anton Paar, Austria) with a 9 mm diameter, 2° cone and plate geometry. The hydrogels (n = 5/group) were synthesized and swollen overnight prior to loading between the cone and plate, after which the measuring system was lowered to a 39 μm gap. Initial strain amplitude sweeps were performed at an angular frequency of 10 rad s^{-1} to determine the linear viscoelastic range of the hydrogel. Oscillatory frequency sweeps were then used to examine the storage and loss moduli (ω= 1–10 rad s^{-1}) at a strain of 1.5%.

2.2.3. Gel degradation studies—PEG gels (500 μL) were fabricated as described above. RGD was labeled by incubation with AlexaFluor647-NHS ester (Thermo Fisher, Carlsbad, CA) for 30 min. Gels were washed in excess DPBS after gelation to remove unbound

AlexaFluor647. Gels were incubated at 37 °C in 0.5 U/mL collagenase type I (Roche, Indianapolis, IN) in DPBS and fluorescence measured using an IVIS SpectrumCT (Perkin Elmer, Waltham, MA) at specified time points. Analysis of gel area was performed using ImageJ/FIJI after signal thresholding at 30% maximum signal to remove background noise.

2.2.4. Gel permeability studies—PEG gels (500 μL) cross-linked with PEGDT were fabricated as described above. Alginate gels (500 μL) were prepared by exposing 1.6% alginate (UP MVG, NovaMatrix, Sandvika, Norway) solution in a 48-well plate to a 1.5% $BaCl_2$-MOPS cross-linking solution (10 mM MOPS, 62 mM NaCl, 3 mM KCl, 0.20 mM Tween-20, 50 mM $BaCl_2 \cdot 2\ H_2O$, and pH 7.4 (adjusted with 6 M NaOH)). Gels were rinsed in DPBS prior to submerging in 3 mL of 0.15 mg/mL FITC-dextran solutions (10 kDa or 150 kDa) or 0.015 mg/mL FITC-insulin or FITC-IgG solutions in DPBS in a 6-well plate for up to 18 h at 37 °C. Fluorescence intensity readings were taken using an IVIS SpectrumCT. Prior to reading, gels were rinsed in DPBS and mounted on glass slides.

2.3. In vitro characterization of islet viability and function

All animal experiments were performed with the approval of the Georgia Tech Animal Care and Use Committee within the guidelines of the Guide for the Care and Use of Laboratory Animals. For islet isolation, male Lewis rats were anesthetized via ketamine (100 mg/kg)/ xylazine (10 mg/kg) (Henry Schein, Melville, NY) and euthanized via exsanguination prior to bile duct cannulation and pancreas perfusion with a solution of collagenase (153.8 μg/mL, Roche), thermolysin (5 μg/mL, Roche), and DNase (100 μg/mL) in sterile Hanks balanced salt solution. Pancreata were digested in 37 °C bath prior to Ficoll (Mediatech, Manassas, VA) density purification (1.11, 1.096, 1.069, 1.037 g/mL) of the islet layer. Islets were counted by the dithizone staining islet equivalent method [29] on the following day immediately prior to encapsulation in hydrogels. Islets were cultured in CMRL-1066 supplemented with 10% fetal bovine serum, 1% penicillin/streptomycin, 1% L-glutamine, 25 mM HEPES. To form islet-containing gels, islets were suspended in PEG-RGD macromer prior to mixing with the cross-linking solution to form the hydrogel. For the 6-day adhesive peptide study, 150 IEQ were encapsulated in 100 μL gels and used for live/dead and glucose-stimulated insulin release (GSIR) assay. Gels were incubated in live/dead solution containing 1 μL/mL each of Calcein-AM (Thermo Fisher) and TOTO-3-iodide (Thermo Fisher) in DPBS. For GSIR, gels were incubated for 1 h intervals sequentially in 3 mM, 3 mM, 16 mM, and 3 mM D-glucose-containing Krebs buffer. For the 48 h study evaluating full scale macrodevices, 4000 IEQ were encapsulated in 500 μL gels. Gels were cut into pieces: one quarter of each was used for live/dead staining and GSIR. Gels were incubated in live/dead solution containing 1 μL/mL each of Calcein-AM and TOTO-3-iodide in DPBS prior to confocal imaging. For GSIR, gels were incubated for 2 h intervals sequentially in 3 mM, 3 mM, 16 mM, and 3 mM D-glucose-containing Krebs buffer to account for diffusion constraints of larger constructs.

2.3.1. COMSOL finite element analysis—The model was implemented in COMSOL Multiphysics 5.2a (COMSOL, Burlington, MA) and solved as a time-dependent (transient) problem, using the Transport of Diluted Species module, allowing intermediate time steps for the solver. Parameters used in the model are summarized in Table 1. 3D models were

constructed using a diffusion-only module with a boundary condition of ambient 0.2 mM O_2 and islet oxygen consumption rate of 100 nmole O_2 per mg DNA per minute [30], resulting in a gel OCR for 4000 IEQ indicated in Table 1. Diffusion was assumed to be governed by the generic diffusion equation in its non-conservative formulation (incompressible fluid):

$$\frac{\partial c_i}{\partial t} + \nabla \cdot (-D_i \nabla c_i) = R_i \quad \text{Equation 1}$$

where c denotes the concentration, D the diffusion coefficient of the species of interest, R the reaction rate, and ∇ the nabla operator $\left(\nabla = \boldsymbol{i}\frac{\partial}{\partial x} + \boldsymbol{j}\frac{\partial}{\partial y} + \boldsymbol{k}\frac{\partial}{\partial z}\right)$.

2.4. In vivo characterization of gel degradation

PEG gels (500 μL) were fabricated in the proportions described above. RGD was labeled by incubation with AlexaFluor 647 NHS ester for 30 min. Gels were washed in excess DPBS after gelation to remove unbound fluorescent dye. For rat omentum transplants, rats were anesthetized with 2% isoflurane. A midline incision was made in the abdominal wall, the omentum exposed, draped, and spread on pre-wet sterile gauze. Gels were centered on the omentum, and the omentum wrapped carefully around the gel. To retain the omentum around the graft but to minimize suturing of the omental tissue, which can induce inflammation and a foreign body response, a PEG-based sealant was applied to the folded tissue, i.e. 30 μL of 10% PEG-MAL functionalized with 1.0 mM RGD and cross-linked via VPM peptide. The omentum was then gently replaced into the abdominal cavity prior to peritoneal closure with sutures and skin closure with staples. For subcutaneous transplants, an incision was made dorsally adjacent to the spine and sufficient connective tissue cleared to allow insertion of a pre-cast gel prior to closure via surgical staples.

2.5. Characterization of vascularized gel layer

For analysis of the impact of the vasculogenic layer, the same omental transplant procedure was followed as outlined above, except the device was coated with either a vasculogenic (VEGF, Thermo Fisher) or control PEG (5% PEG-MAL, 20 kDa, 1.0 mM RGD) with gelation *in situ*. To coat the implant, 70 μL of vasculogenic or control coating was added to the omentum tissue and the macrodevice was immediately placed on top. An additional 140 μL of vasculogenic or control PEG was then added to coat the top and sides of the implant. The omentum was wrapped around the graft and sealed in a manner identical to that described above. After 4 weeks, anesthetized recipients were perfused with 200 μL of AlexaFluor488-conjugated tomato lectin (Vector Labs, Burlingame, CA) via the carotid artery. Lectin was allowed to circulate for 15 min prior to euthanasia and vascular flushing with saline. Grafts were explanted and fixed in 10% formalin. Images (3–5 per graft) were taken via confocal microscopy and analyzed for vascular characteristics using ImageJ/FIJI. 8-bit images were thresholded to remove background fluorescent signal prior to skeletonization and analysis via the “Analyze skeleton” macro plugin.

2.6. In vivo islet viability syngeneic transplant

Diabetes was induced in female Lewis rats via intraperitoneal injection of streptozotocin (65 mg/kg) in sodium citrate buffer (30 mg/mL, pH 4.5) at least one week prior to the scheduled transplantation date. Animals with at least two consecutive blood glucose readings above 350 mg/dL were used as islet transplant diabetic recipients. The day before transplantation, islets were isolated as described above. Islets were counted by dithizone staining islet equivalent method immediately before macroencapsulation hydrogel fabrication and 4000 IEQ were loaded within each construct. Constructs were transplanted within 2 h of fabrication. Vasculogenic or control (no VEGF) degradable coatings were added to selected islet-encapsulating macrodevices (PEG-RGD, 500 μL), as described above (n = 4/group). After 4 weeks, grafts were explanted, sectioned at the midline using surgical scissors, and incubated for 15 min in live/dead solution prior to whole mounting and confocal imaging. A minimum of 4 images per animal were analyzed using ImageJ/FIJI to quantify live and dead fluorescence within regions of interest drawn around islets to eliminate background or omentum tissue fluorescence contributions.

2.6.1 Histological evaluation of islet grafts—For insulin staining, formalin fixed grafts were dissected to isolate thin pieces of the enclosed macrodevice. Gel pieces were placed on glass slides and permeabilized (1 h), blocked (10% goat serum, 1 h), and incubated with primary (guinea pig anti-insulin, DAKO, Santa Clara, CA), and secondary (goat anti-guinea pig AF 594, Thermo Fisher) antibodies sequentially for 1 h each at room temperature. For H&E and leukocyte immunohistochemistry, whole fixed grafts were incubated in 30% sucrose solution overnight at 4°C prior to infiltration with OCT embedding medium under vacuum for 1 h. OCT embedded grafts were frozen in a bath of 2-methylbutane submerged in liquid nitrogen and stored at −80°C until sectioning. 15–20 μm sections were mounted on slides prior to H&E staining using an automated stainer. Sections were sequentially stained after permeabilization and blocking as above for CD45 (Abcam [ab10558], Cambridge, MA) and CD68 (Abcam [ab125212]), with secondary goat anti-rabbit AF594 (Thermo Fisher).

2.6.2 COMSOL modeling of in vivo study—The model was implemented as described in Method section 2.3.1 with the following modifications. The oxygen tension at the boundary was modified using the literature values for omentum arterial oxygen tension (0.1 mM) and non-vascularized intraperitoneal tissue oxygen concentration (0.05 mM) [31], and experimentally determined values for vascular density obtained in the vascularization study (Table 2). The *in vivo* oxygen profile within these macrodevices was then recalculated.

2.7. Statistics

Rheometry data, *in vitro* 48 h GSIR, vascularization study branch length and branch/junction numbers, and islet *in vivo* viability average area and percent islet area were analyzed by two-way ANOVA with Sidak's multiple comparison test. *In vitro* and *in vivo* gel degradation were analyzed by two-way ANOVA with Tukey's multiple comparison test. Diffusion studies analyzed by one-way ANOVA with Tukey's multiple comparison test. Six-day *in vitro* GSIR was analyzed by one-way ANOVA with Dunn's multiple comparison test. 48 h live/dead staining was analyzed by two-way ANOVA. Total vessel length was analyzed by

Student's t-test. Blood glucose and body weight were evaluated by two-way repeated measures ANOVA.

3. Results and Discussion

3.1. Design and in vitro characterization of synthetic PEG-based macroencapsulation device

In the pursuit of a synthetic hydrogel macroencapsulation device capable of long-term *in vivo* containment of encapsulated cells, we sought to design a mechanically and proteolytically stable device with comparable permeability characteristics to traditional micro-scale encapsulation materials (e.g., alginate). To examine non-degradable gel mechanical stability characteristics, synthetic PEG hydrogels were fabricated using the PEG-maleimide macromer and the synthetic cross-linker PEGDT (PEG/PEGDT) at different polymer densities (5.0 and 7.0 wt %) and assessed via rheometry (Fig. 2a and b). For comparison, PEG hydrogels cross-linked with proteolytically degradable peptide cross-linkers VPM (PEG/VPM) or GDQ (PEG/GDQ) were also characterized. Overall, the storage modulus increased with an increase in polymer density (Fig. 2a), resulting in a modest decrease in calculated mesh size (Fig. 2b), with the greatest effect observed for VPM and PEGDT cross-linkers ($P < 0.05$ and $P < 0.001$, respectively) and no significant effect for the GDQ cross-linker (frequency sweeps shown in Suppl. Fig. 1). As the increased 7.0 wt% PEG/PEGDT gels demonstrated enhanced mechanical stiffness with minimal impact on gel mesh size, this polymer and cross-linking method was used for all subsequent studies.

To investigate gel stability in the presence of proteases, we evaluated the stability of 7.0% PEG macrodevices cross-linked with proteolytically degradable peptide (VPM, GDQ) or synthetic (PEGDT) cross-linkers in the presence of collagenase. Macrodevices designed for rat omentum transplantation (500 μL gels) were functionalized with fluorescently labeled RGD peptide prior to fabrication and exposure to collagenase digestion. To quantify gel degradation, gels were imaged daily with an IVIS SpectrumCT (Fig. 2c), and the area of remaining gel was calculated using a threshold minimum of 30% of maximum signal to eliminate edge noise (Fig. 2d). Gels cross-linked with protease-degradable peptides VPM and GDQ exhibited susceptibility to collagenase, with complete degradation of gels cross-linked with GDQ or VPM within 1 and 8 days, respectively. Whereas earlier publications indicated that the GDQ peptide sequence exhibits low susceptibility to specific proteases (e.g. trypsin [32] and matrix metalloproteinase-1 [33]), more recent studies report higher protease sensitivity [34, 35]. As expected, gels cross-linked with PEGDT demonstrated no detectable protease susceptibility, maintaining stable gel signal and area throughout the observation period. These data suggest that PEGDT is the most suitable cross-linker for long term macroencapsulation device stability *in vivo*.

Permeability is a crucial material characteristic for islet immunoisolation, because the hydrogel network must allow insulin (7 kDa) and nutrients to readily transverse the material while limiting transport of immunogenic molecules such as IgG (150 kDa). We evaluated the permeability of the PEG/PEGDT macroencapsulation device using model molecules of 10 kDa and 150 kDa FITC-dextran and IVIS Spectrum CT imaging (Fig. 2e), with alginate included as a reference encapsulation material due to its widespread use. As alginate

gelation is achieved via an external agent, resulting macrogels were less controlled in shape and exhibited a more spherical geometry than the targeted disk shape achieved using PEG gels (Fig. 2f, insets), as highlighted in histogram measurements of FITC-dextran signal intensity (Fig. 2f) where alginate gels exhibit a smaller diameter than PEG/PEGDT gels (10 mm and 12 mm diameter, respectively; see Supp. Fig. 3). Because gel height influences fluorescent intensity readings, this variation in geometry resulted in a statistically insignificant increase in fluorescence reading for FITC-dextran in alginate vs. PEG/PEGDT gels (Fig. 2g). For both alginate and PEG/PEGDT gels, 10 kDa FITC-dextran rapidly and uniformly diffused into the gels within 15 min of exposure, with a continued gradual rise over the observation period. Conversely, 150 kDa FITC-dextran signal peaked within 15 min and the higher signal was limited to the gel edges, indicating limited diffusion throughout the gels. Similar trends in permeability were observed for fluorescently labeled insulin and IgG (Supp. Fig. 2). Taken together, the data indicates that 7.0% PEG/PEGDT gels exhibit adequate mechanical and protease stability *in vitro*, while maintaining molecular permeability comparable to alginate, the most broadly used material in islet encapsulation.

3.2. Characterization of in vitro islet performance in macroencapsulation device

Maintenance of islet viability and function is a central feature of macroencapsulation device design. In addition to the capacity for cross-linking under physiological conditions, synthetic PEG-maleimide hydrogels enable facile functionalization of the macromer with cysteine-terminated peptides, allowing optimization of the hydrogel matrix for encapsulation of specific cell types. As such, we first evaluated whether the incorporation of an adhesive peptide within our synthetic hydrogel maintains encapsulated islet function over multiple days in culture. Whereas short term pilot studies did not show significant differences in islet viability, we hypothesized that longer term culture would demonstrate the importance of adhesive peptide inclusion because of prolonged stress to the islets. Islets were encapsulated within synthetic PEG hydrogels containing either RGD or scrambled, non-adhesive RDG peptide (control), and either degradable (VPM) or synthetic (PEGDT) cross-linker, and unencapsulated (free) or alginate-encapsulated islets were used as controls. After 6 days in culture, islets were evaluated for viability via live/dead imaging (Fig. 3a), and function, as measured via the glucose-stimulated insulin response assay (GSIR) (Fig. 3b). Islets exhibited comparable live/dead staining across all groups. In contrast, notable differences in the response of the islets to a glucose challenge, presented as the stimulation index, were observed. As expected, the confinement of islets within a macroscale PEG hydrogel resulted in decreased insulin responsiveness to a glucose challenge, when compared to free islets ($P < 0.05$). The inclusion of the RGD peptide, however, resulted in a stimulation index equivalent to unencapsulated islets. Furthermore, RGD-presenting PEG hydrogels exhibited comparable stimulation index to the alginate reference. These data indicate that inclusion of RGD adhesive peptide contributes to maintenance of islet function in culture within the synthetic PEG macrodevice. For all subsequent studies, PEG hydrogels were functionalized with RGD.

Islet viability and function was evaluated *in vitro* using macroencapsulation hydrogels at the scale required for transplantation into a rat model (i.e. 500 μL). Alginate macrogels were used as a control material; however, it should be noted that their inherent variable material

properties resulted in different gel geometries (see Supp. Fig. 3). Islets were encapsulated in PEG/PEGDT or alginate hydrogels and cultured 48 h prior to live/dead staining (Fig. 4a–c) and GSIR (Fig. 4f–g). Gross observation of low magnification live/dead images (Fig. 4a) revealed differences in the patterns of islet viability within the hydrogels, with PEG/PEGDT gels exhibiting more elevated islet viability near the center of the gels than alginate controls. This observation was confirmed with higher magnification images of encapsulated islets (Fig. 4b). Quantification of live/dead signal intensity within the gels demonstrated an increase in dead signal within alginate gels as the distance from the gel edge increased (Fig. 4c). The difference in viability between alginate and PEG/PEGDT gels was unexpected, considering their comparable diffusion kinetics (Fig. 2 and Supp. Fig. 2). With comparable permeability, the overall 3-D geometry of the macrodevices may play a role, which may result in variable diffusional lengths within the gels. Given the high oxygen demand of islets, even modest increases in diffusional lengths can result in decreased oxygen availability and subsequent islet viability. To evaluate this, finite element analysis was used to evaluate oxygen profiles within cylindrical or spherical gels over 48 h (Fig. 4d–e). We found that oxygen diffusion profiles (Fig. 4d) matched the distribution of live/dead cells (Fig. 4a), and a plot of these profiles (Fig. 4e) matched the profile of dead staining (Fig. 4c). Finally, we evaluated insulin responsiveness to glucose of encapsulated islets (Fig. 4f) where both the stimulation index (Fig. 4g) and total insulin release (Fig. 4h) exhibited no significant differences between alginate and PEG/PEGDT groups. While alginate encapsulated cells exhibited decreased viability within the central region of the gels, it is likely that islets nearer the periphery of the gels have a greater influence on insulin measurements in Fig. 4g, resulting in non-significant differences in insulin measurements between the two groups. Taken together, these data show that the engineered PEG hydrogel macrodevice supports islet viability and function *in vitro,* contributed in part by the highly controlled cylindrical geometry of synthetic PEG macrodevices.

3.3. Characterization of synthetic PEG macroencapsulation device degradation and remodeling in vivo

After establishing the proteolytic stability of macroencapsulation hydrogels *in vitro* (Fig 2), it was critical to confirm the stability of the device *in vivo*, as the *in vitro* model cannot fully recapitulate the tissue microenvironment and its long-term response to a persistent material. To examine PEG gel stability *in vivo*, we fabricated gels containing fluorescently labeled RGD and cross-linked with synthetic (PEGDT) or proteolytically degradable cross-linkers (VPM, GDQ), implanted the gels in either the omentum (Fig. 5a, c, e) or subcutaneous space (Fig. 5b, d, f) of rats, and monitored the *in vivo* fluorescent signal via an IVIS SpectrumCT over a period of 14 weeks. This modality allowed for the quantification of signal intensity (Fig. 5a–d) and gel area (Fig. 5e, f) during the observation window. The high mobility of the intraperitoneal omental tissue, in conjunction with artifacts produced by other abdominal organs obstructing the transplanted gel, produced high variability in images obtained of omentum-transplanted gels (Fig. 5a). In contrast, subcutaneously transplanted gels exhibited low mobility and lower potential for imaging artifacts (Fig. 5b), permitting more reliable measurements. Signal intensity measurements of subcutaneous transplants were comparable to relative degradation rates observed *in vitro* (Fig. 5d), while the omentum signal intensity (Fig. 5c) exhibited considerable variability. Interestingly, whereas the subcutaneous gel

signal intensity followed trends consistent with the *in vitro* results (Fig. 5d), gel area for all constructs decreased over the observation period (Fig. 5f), with PEGDT-cross-linked gels exhibiting 50% original area at week 14 compared to 0% for gels cross-linked with the peptide cross-linkers. For the omentum transplants, gel area followed expected trends with greater consistency (Fig. 5e), with PEG/PEGDT maintaining gel area while PEG gels with protease-degradable cross-linkers exhibited reduced area over 14 weeks. To confirm IVIS imaging observations, subcutaneous grafts were explanted and imaged for tissue infiltration (Fig. 5g). DAPI staining of infiltrating tissue from the explant extended to the greatest extent in GDQ-cross-linked gels, but was limited to the gel periphery in PEGDT-cross-linked gels. As observed for *in vitro* degradation studies, VPM-cross-linked gels offered a more moderate degradation rate than that observed for GDQ-cross-linked gels. IVIS imaging of explanted gels confirmed the presence of robust fluorescent signal in PEG/PEGDT gels, with diminished signal in PEG/GDQ and PEG/VPM gels in both omentum (Supp. Fig. 4a) and subcutaneous space (Supp. Fig. 4b). Explanted PEG/PEGDT gels exhibited a higher fluorescent signal than the corresponding *in vivo* signal due to lack of signal obstruction by surrounding tissues. Conversely, explanted PEG/PEGDT gels exhibited a lower signal than non-transplanted control gels that lacked any tissue adherence to the surface (Supp. Fig. 4c) making it difficult to conclusively determine by this method whether PEG/PEGDT gels exhibit degradation *in vivo*. Overall, these data provide *in vivo* support that PEGDT cross-linked hydrogels exhibit greater stability than proteolytically degradable peptide cross-linkers.

3.4. Evaluation of degradable vasculogenic layer impact on vascular remodeling on macroencapsulation device surface

With optimization of the PEG core macrogel, the next phase focused on the incorporation of an outer degradable, vasculogenic gel coating to enhance vascularization at the PEG/PEGDT-tissue interface. Our previous work has demonstrated that islet delivery within a vasculogenic degradable hydrogel enhances functional performance of the graft within a vascularized transplant site [26, 27]. This previous work demonstrated that the subcutaneous site is less vascularized than intraperitoneal tissue such as the omentum; therefore all subsequent experiments investigated macrodevice performance within the omentum. In this study, we sought to examine the capacity of our vasculogenic hydrogel to enhance vascularization at the surface of a non-degradable macrodevice, and therefore increase nutrient delivery to encapsulated cells. A thin coating (~1 mm) of degradable hydrogel with (VEGF) or without (control) vasculogenic factor was added to PEG/PEGDT macroencapsulation devices and the engraftment within the omentum of Lewis rats was evaluated (Fig. 6a). After 4 weeks post-transplant, functional vasculature at the interface of the device was evaluated via confocal whole mount and cross-sectional imaging of lectin perfused vessels (Fig. 6b–c, respectively). To quantify vascularization, whole mount images were analyzed for vessel branch and junction number (Fig. 6d), average and maximum branch length (Fig. 6e), and total vessel length (Fig. 6f). Statistical analyses of all metrics found that localized VEGF delivery via a degradable hydrogel coating at the surface of PEG/PEGDT macroencapsulation device significantly enhanced vascular ingrowth ($P < 0.05$) and density ($P < 0.005$). Increasing vascular density at the surface of the macroencapsulation

hydrogel may contribute to greater oxygen tension at the surface and thus within the interior of the device, potentially facilitating improved viability of cells delivered within the device.

3.5. Impact of vasculogenic layer on macroencapsulated islet survival in syngeneic diabetic recipients

To assess if enhanced vascularization due to a vasculogenic coating on the macroencapsulating hydrogel resulted in improved transplant efficacy, syngeneic islets were encapsulated within RGD-containing PEG/PEGDT macroencapsulation devices and delivered to the omentum of diabetic Lewis rats with a degradable hydrogel layer with (VEGF) or without (control) vasculogenic factor. Non-fasting blood glucose (Fig. 7a) and body weight (Fig. 7b) was monitored up to 4 weeks post-transplant. At 4 weeks post-transplant, macrodevices were explanted and sectioned at the midline (Fig. 7c) prior to live/dead staining and whole-mount imaging at low (Fig. 7c) and high (Fig. 7d) magnification, with images obtained at both the edge of the gel proximal to omental tissue and at the center of the gel, distant from omental tissue. Live islets were observed at a greater frequency within rats receiving PEG gels with the VEGF-gel layer compared to controls (Fig. 7e), with the greatest effect observed at the center of the gels (Fig. 7f). Additionally, both groups exhibited insulin-positive islets at the experimental end-point (Supp. Fig. 5a).

To gather insight on whether the increased survival could be attributed to greater oxygen tension at the surface of the VEGF gels, finite element analysis was used to model oxygen distribution within the gels at 28 days post-transplant. Using calculations of increased vascular density induced by the VEGF gel layer and published oxygen tension values for intraperitoneal tissue and arterial vessels, the average oxygen concentrations of 0.064 mM and 0.072 mM for the outer boundary of control and VEGF-delivering macrodevices, respectively, were derived. Using these values, we predicted a denser region of oxygen deprivation within control macrodevices, when compared to macrodevices coated with VEGF-delivering gels (Fig. 7g), with an average central oxygen tension within the gels of 0.018 mM and 0.027 mM for control and VEGF-layer macrodevices, respectively (Fig. 7h). Collectively, these data indicate that increases in macrodevice surface vascularization have the capacity to improve encapsulated islet viability. While this improved viability did not impact non-fasting blood glucose or body weight in this study, we hypothesize that islet loading optimized for the oxygen gradient within the device could demonstrate functional improvement. Future studies will explore the capacity of enhanced vascularization to augment *in vivo* device performance on an optimized islet loading.

Prior work has addressed inadequate oxygenation of islet encapsulating macrodevices by direct supplementation through an external port [14], but this strategy relies on patient compliance for daily oxygen replenishment. Other groups have explored macrodevice prevascularization to improve islet survival, strategies which require multiple procedures to achieve the desired outcome [16]. In contrast, our strategy of local modulation of oxygen tension through improved device vascularization can be accomplished through a single procedure, eliminating reliance on long-term patient compliance. Indeed, the omentum transplant and *in situ* gelation of the vasculogenic hydrogel layer can be achieved through laparoscopic techniques, potentially resulting in a minimally invasive procedure. While it is

unclear why the islet loading used in this study was insufficient to achieve euglycemia, macrodevices for islet delivery typically require a greater number of islets to achieve normoglycemia than alternative strategies, indicating a greater islet loading may be required to achieve complete normoglycemia [14, 16]. Future studies will investigate the optimal islet loading within the hydrogel macrodevice to achieve stable and long-term function.

Although it is common for fibrosis to occur with VEGF-mediated angiogenesis [36], our previous work [26] indicated that controlled delivery of VEGF through degradable hydrogels does not result in heightened leukocyte response. Additionally, H&E staining (Supp. Fig. 5b) of omentum-transplanted macrodevices, and immunohistochemistry (Supp. Fig. 5c) targeting leukocytes (CD45), and specifically macrophages (CD68), does not indicate a difference in fibrotic response between control and VEGF-laden gels.

The delivery strategy of a single macroencapsulation device containing insulin-producing cells, as well as targeting our hydrogel delivery to a contained site such as the omentum, enhances the safety of encapsulated islet transplantation by maximizing the retrievability of the graft. As such, this strategy may present a safe strategy for delivering alternatively sourced insulin-producing cells, such as stem cell-derived or xenogeneic beta cell sources. Limited donor tissue availability has long presented a challenge to translating cell therapy as a treatment for insulin-dependent patients, and the development of a fully contained and retrievable graft may open the door to translation of alternative cell sources as a solution to pancreatic islet shortages.

4. Conclusion

We present a synthetic, non-degradable hydrogel macrodevice designed to encapsulate and deliver islets to the omentum. Our synthetic hydrogel macrodevice demonstrates mechanical and proteolytic stability *in vitro* and *in vivo* and supports islet viability *in vitro.* Furthermore, we show that device supplementation with a vasculogenic hydrogel coating improves encapsulated islet viability over control gels. Future studies will explore the optimal islet density for full restoration of normoglycemic in rodent models, as well as evaluate the degree of immunoprotection imparted by abrogation of direct antigen recognition alone in an allogeneic model.

Supplementary Material

Refer to Web version on PubMed Central for supplementary material.

Acknowledgments

The authors thank the Juvenile Diabetes Research Foundation (JDRF) for their support through the encapsulation consortium (3-SRA-2015-38-Q-R) and Postdoctoral Fellowship Award, and the National Institutes of Health (NIH, U01 AI132817) for their financial support.

References

1. Centers for Disease Control and Prevention. National diabetes statistics report, 2017. Atlanta, GA: Centers for Disease Control and Prevention, US Dept of Health and Human Services; 2017.

2. Tao B, Pietropaolo M, Atkinson M, Schatz D, Taylor D. Estimating the cost of type 1 diabetes in the US: a propensity score matching method. PLoS One. 2010; 5(7):e11501. [PubMed: 20634976]
3. Centers for Disease Control and Prevention. National diabetes statistics report, 2011. Atlanta, GA: Centers for Disease Control and Prevention, US Dept of Health and Human Services; 2011.
4. Calafiore R. Perspectives in pancreatic and islet cell transplantation for the therapy of IDDM. Diabetes Care. 1997; 20(5):889–896. [PubMed: 9135962]
5. Shapiro AJ, Lakey JR, Ryan EA, Korbutt GS, Toth E, Warnock GL, Kneteman NM, Rajotte RV. Islet transplantation in seven patients with type 1 diabetes mellitus using a glucocorticoid-free immunosuppressive regimen. N Engl J Med. 2000; 343(4):230–238. [PubMed: 10911004]
6. Ludwig B, Reichel A, Steffen A, Zimerman B, Schally AV, Block NL, Colton CK, Ludwig S, Kersting S, Bonifacio E. Transplantation of human islets without immunosuppression. Proc Natl Acad Sci USA. 2013; 110(47):19054–19058. [PubMed: 24167261]
7. Ricordi C, Strom TB. Clinical islet transplantation: advances and immunological challenges. Nat Rev Immunol. 2004; 4(4):259–268. [PubMed: 15057784]
8. Giraldo JA, Weaver JD, Stabler CL. Enhancing clinical islet transplantation through tissue engineeering strategies. J Diabetes Sci Technol. 2010; 4(5):1238–1247. [PubMed: 20920446]
9. Orive G, Hernández RM, Gascón AR, Calafiore R, Chang TM, De Vos P, Hortelano G, Hunkeler D, Lacík I, Shapiro AJ. Cell encapsulation: promise and progress. Nat Med. 2003; 9(1):104–107. [PubMed: 12514721]
10. de Vos P, Lazarjani HA, Poncelet D, Faas MM. Polymers in cell encapsulation from an enveloped cell perspective. Adv Drug Deliv Rev. 2014; 67:15–34. [PubMed: 24270009]
11. O'sullivan ES, Vegas A, Anderson DG, Weir GC. Islets transplanted in immunoisolation devices: a review of the progress and the challenges that remain. Endocr Rev. 2011; 32(6):827–844. [PubMed: 21951347]
12. Schweicher J, Nyitray C, Desai TA. Membranes to achieve immunoprotection of transplanted islets. Front Biosci. 2014; 19:49.
13. Vos, Pd, Andersson, A., Tam, S., Faas, M., Halle, J. Advances and barriers in mammalian cell encapsulation for treatment of diabetes, Immunol. Endocr Metab Agents Med Chem. 2006; 6(2): 139–153.
14. Tuch BE, Keogh GW, Williams LJ, Wu W, Foster JL, Vaithilingam V, Philips R. Safety and viability of microencapsulated human islets transplanted into diabetic humans. Diabetes Care. 2009; 32(10):1887–1889. [PubMed: 19549731]
15. Juang JH, Bonner-Weir S, Ogawa Y, Vacanti JP, Weir GC. Outcome of subcutaneous islet transplantation improved by polymer device. Transplantation. 1996; 61(11):1557–1561. [PubMed: 8669096]
16. Pileggi A, Molano RD, Ricordi C, Zahr E, Collins J, Valdes R, Inverardi L. Reversal of diabetes by pancreatic islet transplantation into a subcutaneous, neovascularized device. Transplantation. 2006; 81(9):1318–1324. [PubMed: 16699461]
17. Wang W, Gu Y, Hori H, Sakurai T, Hiura A, Sumi S, Tabata Y, Inoue K. Subcutaneous transplantation of macroencapsulated porcine pancreatic endocrine cells normalizes hyperglycemia in diabetic mice. Transplantation. 2003; 76(2):290–296. [PubMed: 12883181]
18. Suzuki K, Bonner-Weir S, Trivedi N, Yoon KH, Hollister-Lock J, Colton CK, Weir GC. Function and survival of macroencapsulated syngeneic islets transplanted into streptozotocin-diabetic. Transplantation. 1998; 66(1):21–28. [PubMed: 9679817]
19. Sato Y, Endo H, Okuyama H, Takeda T, Iwahashi H, Imagawa A, Yamagata K, Shimomura I, Inoue M. Cellular hypoxia of pancreatic β-cells due to high levels of oxygen consumption for insulin secretion in vitro. J Biol Chem. 2011; 286(14):12524–12532. [PubMed: 21296882]
20. Dionne KE, Colton CK, Lyarmush M. Effect of hypoxia on insulin secretion by isolated rat and canine islets of Langerhans. Diabetes. 1993; 42(1):12–21. [PubMed: 8420809]
21. Balamurugan A, Gu Y, Tabata Y, Miyamoto M, Cui W, Hori H, Satake A, Nagata N, Wang W, Inoue K. Bioartificial pancreas transplantation at prevascularized intermuscular space: effect of angiogenesis induction on islet survival. Pancreas. 2003; 26(3):279–285. [PubMed: 12657955]

22. Sakurai T, Satake A, Sumi S, Inoue K, Nagata N, Tabata Y, Miyakoshi J. The efficient prevascularization induced by fibroblast growth factor 2 with a collagen-coated device improves the cell survival of a bioartificial pancreas. Pancreas. 2004; 28(3):e70–e79. [PubMed: 15084987]

23. Pedraza E, Coronel MM, Fraker CA, Ricordi C, Stabler CL. Preventing hypoxia-induced cell death in beta cells and islets via hydrolytically activated, oxygen-generating biomaterials. Proc Natl Acad Sci USA. 2012; 109(11):4245–4250. [PubMed: 22371586]

24. Skrzypek K, Nibbelink MG, Lente J, Buitinga M, Engelse MA, Koning EJ, Karperien M, Apeldoorn A, Stamatialis D. Pancreatic islet macroencapsulation using microwell porous membranes. Sci Rep. 2017; 7(1):9186. [PubMed: 28835662]

25. Trivedi N, Steil G, Colton C, Bonner-Weir S, Weir G. Improved vascularization of planar membrane diffusion devices following continuous infusion of vascular endothelial growth factor. Cell Transplant. 2000; 9(1):115–124. [PubMed: 10784073]

26. Weaver JD, Headen DM, Aquart J, Johnson CT, Shea LD, Shirwan H, García AJ. Vasculogenic hydrogel enhances islet survival, engraftment, and function in leading extrahepatic sites. Sci Adv. 2017; 3(6):e1700184. [PubMed: 28630926]

27. Phelps EA, Headen DM, Taylor WR, Thule PM, Garcia AJ. Vasculogenic bio-synthetic hydrogel for enhancement of pancreatic islet engraftment and function in type 1 diabetes. Biomaterials. 2013; 34(19):4602–11. [PubMed: 23541111]

28. Phelps EA, Templeman KL, Thulé PM, García AJ. Engineered VEGF-releasing PEG–MAL hydrogel for pancreatic islet vascularization. Drug Deliv Transl Res. 2013; 5(2):125–136.

29. Kissler H, Niland J, Olack B, Ricordi C, Hering B, Naji A, Kandeel F, Oberholzer J, Fernandez L, Contreras J. Validation of methodologies for quantifying isolated human islets: an islet cell resources study. Clin Transplant. 2010; 24(2):236–242. [PubMed: 19719726]

30. Papas KK, Bellin MD, Sutherland DE, Suszynski TM, Kitzmann JP, Avgoustiniatos ES, Gruessner AC, Mueller KR, Beilman GJ, Balamurugan AN. Islet oxygen consumption rate (OCR) dose predicts insulin independence in clinical islet autotransplantation. PLoS One. 2015; 10(8):e0134428. [PubMed: 26258815]

31. Golub AS, Barker MC, Pittman RN. PO2 profiles near arterioles and tissue oxygen consumption in rat mesentery. Am J Physiol Heart Circ Physiol. 2007; 293(2):H1097–H1106. [PubMed: 17483242]

32. Babel W, Glanville RW. Structure of human-basement-membrane (type IV) collagen. FEBS J. 1984; 143(3):545–556.

33. Lutolf M, Lauer-Fields J, Schmoekel H, Metters AT, Weber F, Fields G, Hubbell JA. Synthetic matrix metalloproteinase-sensitive hydrogels for the conduction of tissue regeneration: engineering cell-invasion characteristics. Proc Natl Acad Sci USA. 2003; 100(9):5413–5418. [PubMed: 12686696]

34. Patterson J, Hubbell JA. Enhanced proteolytic degradation of molecularly engineered PEG hydrogels in response to MMP-1 and MMP-2. Biomaterials. 2010; 31(30):7836–7845. [PubMed: 20667588]

35. Patterson J, Hubbell JA. SPARC-derived protease substrates to enhance the plasmin sensitivity of molecularly engineered PEG hydrogels. Biomaterials. 2011; 32(5):1301–1310. [PubMed: 21040970]

36. Kreuger J, Phillipson M. Targeting vascular and leukocyte communication in angiogenesis, inflammation and fibrosis. Nat Rev Drug Disc. 2016; 15(2):125.

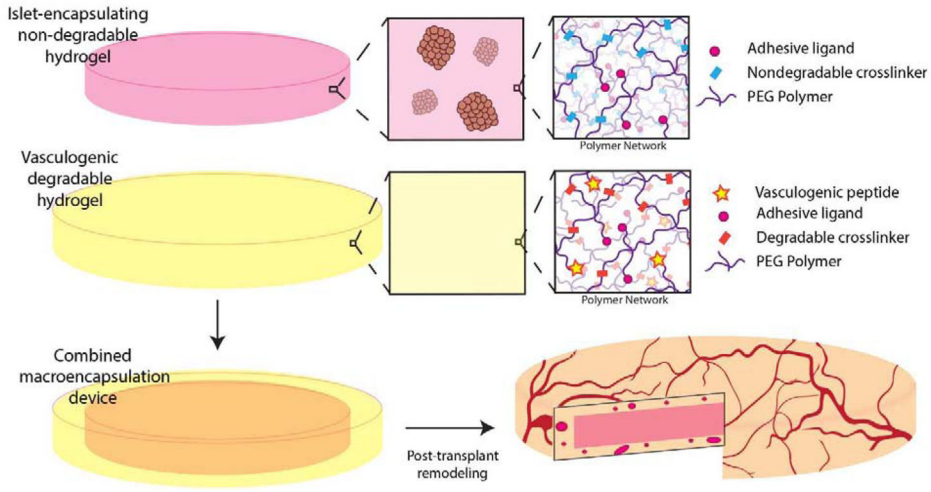

Figure 1. Schematic for synthetic hydrogel macroencapsulation device design

A non-degradable synthetic hydrogel disk is surrounded by a degradable, vasculogenic hydrogel that remodels to promote device vascularization post-transplantation.

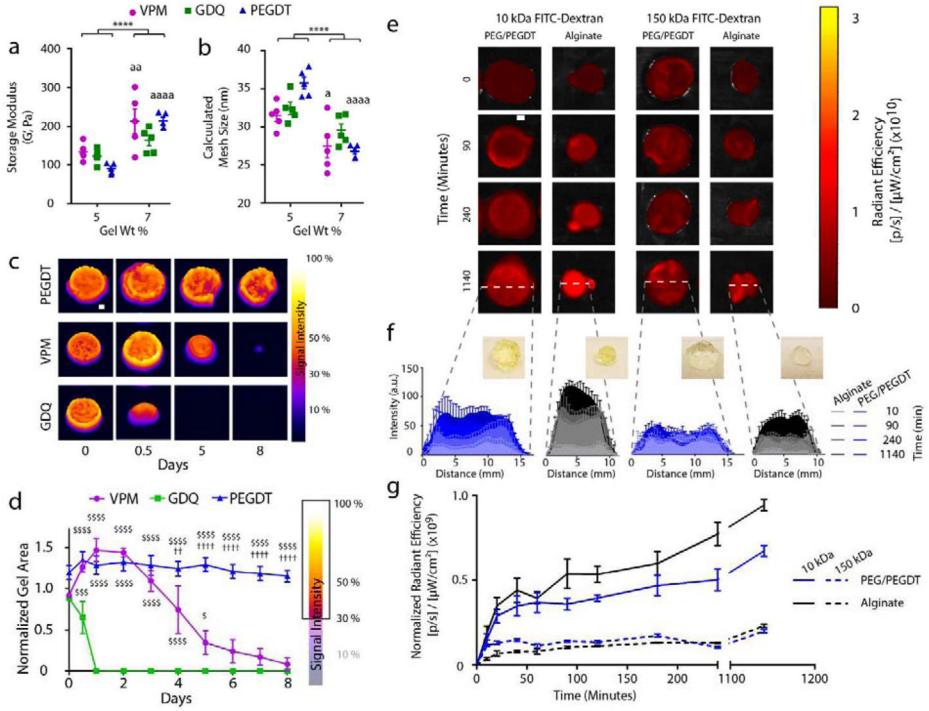

Figure 2. *In vitro* characterization of PEG macrodevice properties

Macrodevice (n = 5/group) formed with degradable or non-degradable cross-linkers were assessed by rheometry to evaluate gel weight percent impact on (a) storage modulus and (b) calculated mesh size. Fluorescently-labeled macrodevices (n = 4/group) cross-linked with non-degradable (PEGDT) and degradable peptides (VPM, GDQ) were assessed for (c) stability and degradation rate via incubation in collagenase and whole-gel IVIS fluorescence imaging and (d) quantification of gel area post-thresholding of fluorescent signal intensity at 30%. (e) Transport kinetics in non-degradable PEG/PEGDT and alginate macrodevices (n = 3/group) were assessed via diffusion of FITC dextrans (10kDa and 150kDa) and temporal IVIS fluorescence imaging of whole gels. (f) Histograms of central cross sections of gels and (g) measurement of radiant efficiency measurements of entire gels normalized to gel cross sectional area demonstrate transport kinetics over time. ^{a} P < 0.05, ^{aa} P < 0.005, ^{aaaa} P < 0.0001 vs 5% gel; **** P < 0.0001. Analysis by 2-way ANOVA with Sidak's multiple comparison test. $ P < 0.05, $$$ P < 0.0005, $$$$ P < 0.0001 vs. GDQ; †† P < 0.005, †††† P < 0.0001 vs. VPM. Analysis by 2-way ANOVA with Tukey's multiple comparison test.

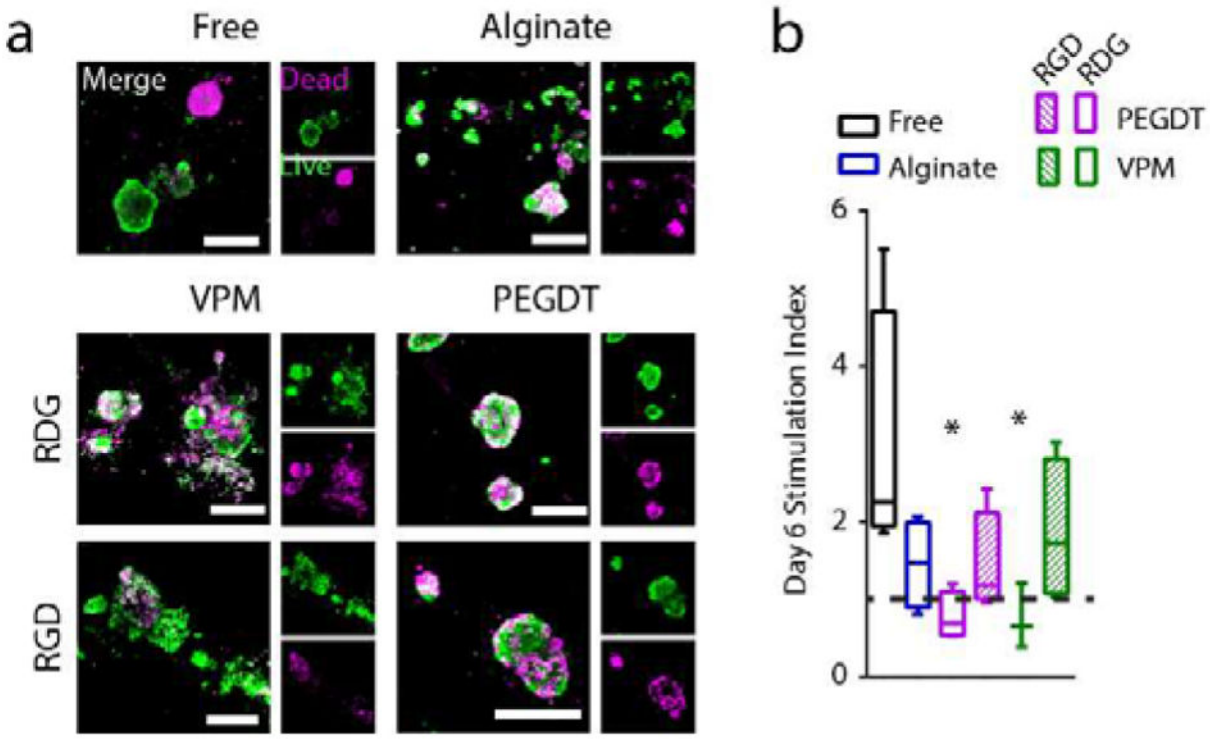

Figure 3. Effect of adhesive peptide on encapsulated islet function in PEG macrodevices

Islets cultured 6 days, either unmodified (free), or in gels cross-linked with degradable peptide (VPM) or non-degradable synthetic monomer (PEGDT), or alginate control gels and evaluated for (a) live/dead and (b) glucose stimulation index. Dashed line indicates high/low ratio of 1.0. * $P < 0.05$ vs free islets (one-way ANOVA with Dunn's multiple comparison test, n = 3–4/group), error bars = SEM, scale bars = 200 μm.

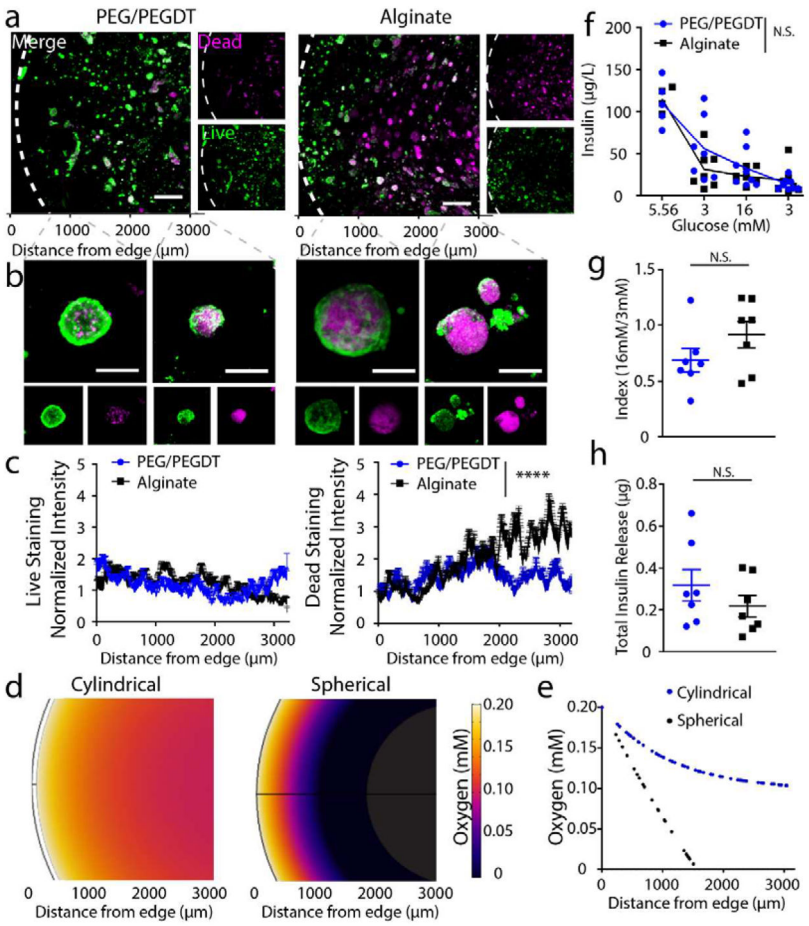

Figure 4. *In vitro* characterization of encapsulated islet viability and function within 500 μL macrodevices

Live/dead imaging at (a) low and (b) high magnification demonstrates islet viability in PEG/PEGDT gels compared to alginate. Swelling of PEG/PEGDT post encapsulation results in lower density of islets within macrodevices, reducing detrimental nutrient gradient compared to non-swelling alginate gels and resulting in improved islet viability throughout PEG/PEGDT gels, as quantified in (c) Live and Dead intensity values normalized to edge values. (d) Gel cross section oxygen distribution profiles and (e) quantitative plot of oxygen concentration within gels demonstrate greater nutrient competition in spherical gels compared to cylindrical disk-shaped gels. (f) Glucose stimulated insulin response assay, (g) index values, and (h) total insulin released demonstrate comparable response between alginate and PEG/PEGDT macrodevices. Live/dead histograms evaluated by repeated measures one-way ANOVA with Sidak's multiple comparison test. GSIR data analyzed by two-way ANOVA with Sidak's multiple comparison test, n = 7/group, data pooled from two separate experiments. Error bars = SEM, scale bars panel A = 500 μm, scale bars panel B = 50 μm. **** $P < 0.0001$ by two-way ANOVA, N.S. = no significance.

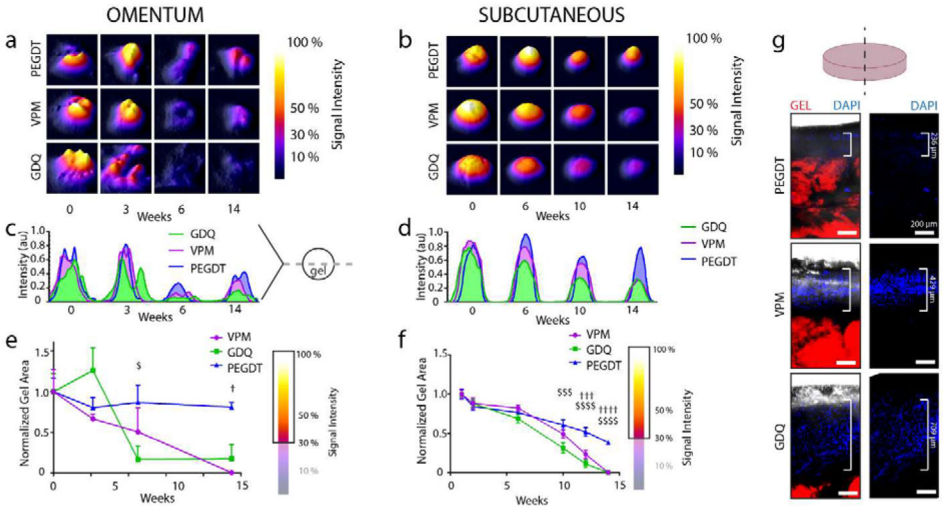

Figure 5. *In vivo* monitoring of PEG hydrogel macroencapsulation device stability comparing non-degradable synthetic (PEGDT) and degradable peptide (VPM, GDQ) cross-linkers

RGD adhesive ligand was fluorescently labeled for *in vivo* tracking of synthetic hydrogels transplanted in the (a, c, e) omentum and (b, d, f, g) subcutaneous space (n = 4/group) of rats. Topographic images of IVIS *in vivo* gel imaging at select time points demonstrate signal stability and remodeling of gel shape for (a) OM and (b) SUBQ implanted gels. Corresponding signal intensity histograms for cross sections of gels in (a) and (b) illustrate fluorescent signal intensity over time for (c) OM and (d) SUBQ implanted gels. Temporal changes in gel area was quantified from IVIS topographic images (A and B) by thresholding signal at 30% intensity and normalization to early time points for both (e) OM and (f) SUBQ implanted gels. (g) Explanted gels demonstrate greater levels of tissue infiltration for degradable cross-linkers (SUBQ). Gel degradation analyzed by two-way ANOVA with Tukey's multiple comparison test. Scale bars = 200 μm. $ $P < 0.05$, $$$ $P < 0.0005$, $$$$ $P < 0.0001$ vs. GDQ; † $P < 0.05$, ††† $P < 0.0005$, †††† $P < 0.0001$ vs. VPM.

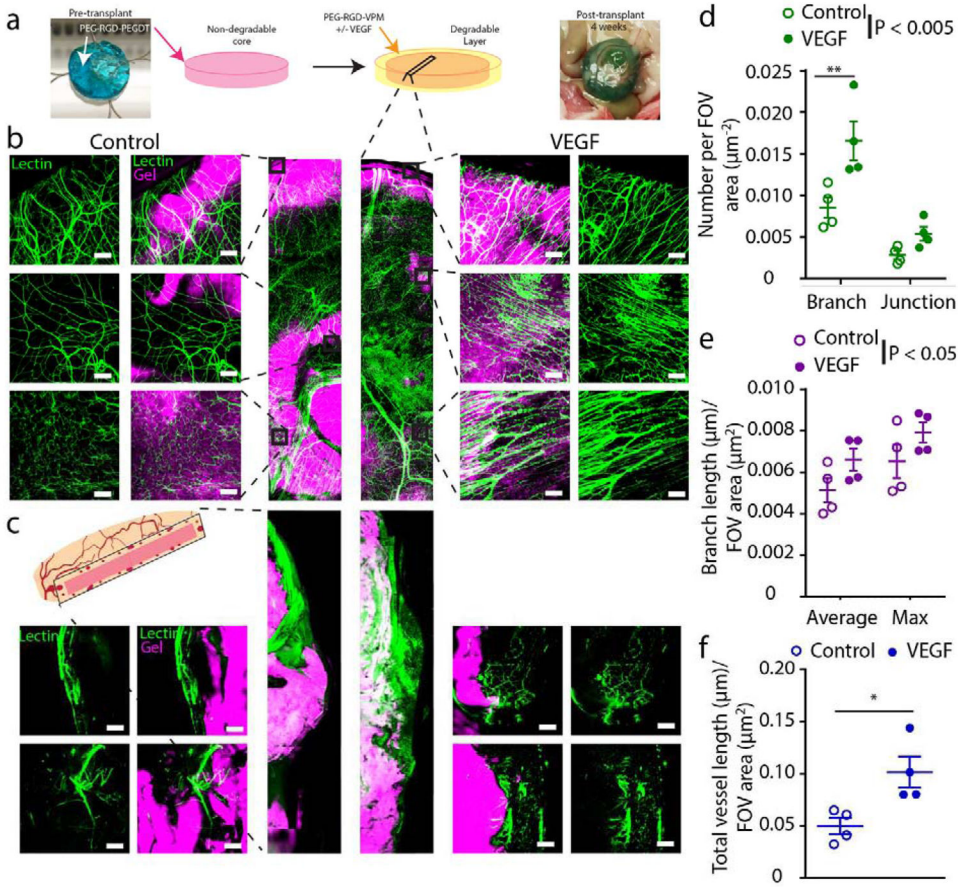

Figure 6. Vascular remodeling of PEG/PEGDT macrodevices transplanted with vasculogenic layer in the omentum

(a) Fluorescently labeled RGD-laden non-degradable macrodevices were transplanted within the omentum of rats with a degradable (VPM) hydrogel layer, either with (VEGF) or without (Control) vasculogenic factor. At 4 weeks post-transplant, subjects were lectin perfused to label functional vasculature (green), and whole mount imaged to visualize degree of (b) surface and (c) cross section vascularization. Surface vascularization was characterized and quantified for number of (d) vessel junctions and branches, (e) average and maximum branch length, (f) and total overall vessel length per field of view (FOV). (n = 4/condition, FOV = 5–8/n). * $P < 0.05$, ** $P < 0.005$. Branch length and branch/junction numbers were analyzed by two-way ANOVA with Sidak's multiple comparison test. Total vessel length analyzed by Student's t-test. Scale bar = 200 μm.

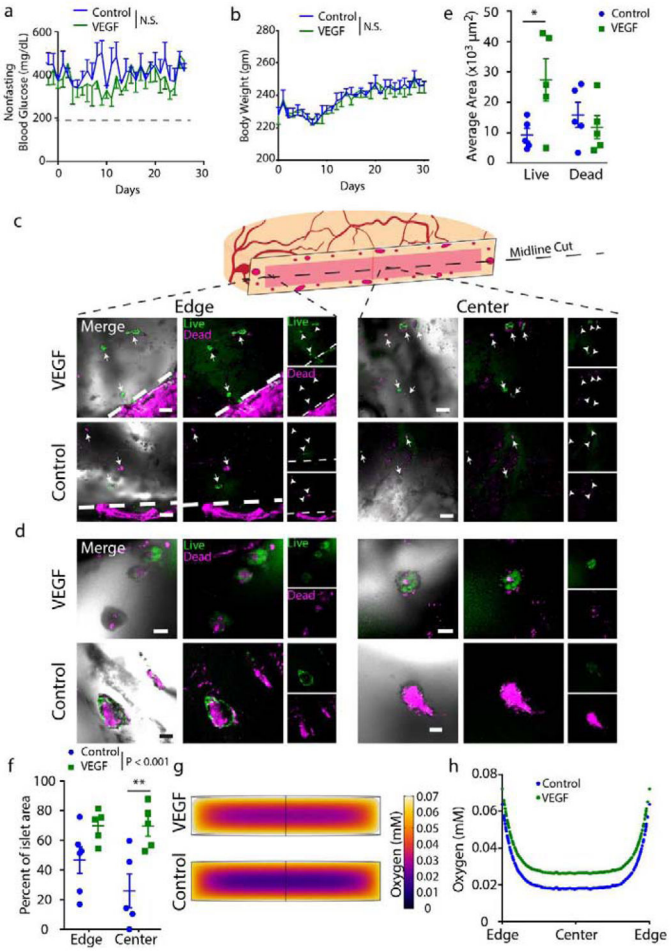

Figure 7. Impact of vasculogenic hydrogel layer on syngeneic PEG/PEGDT macrodevice rat omentum graft viability

Macrodevices (PEG-RGD/PEGDT) containing 4000 syngeneic islet equivalents were transplanted in the omentum with (VEGF) or without (Control) a vasculogenic hydrogel layer. Subjects were monitored for (a) nonfasting blood glucose and (b) body weight. (c, d) After 30 days, grafts were explanted to evaluate viability of encapsulated islets via live/dead staining (c: low magnification; d: high magnification), where (e) quantification of overall graft live/dead area illustrates the impact of macrodevice vascularization via a degradable vasculogenic layer. (f) Evaluation of live islet area percentage at gel edge vs. gel center demonstrates viability distribution between gel edge and center. Finite element analysis (FEA) theoretically predicted spatial variance (g–h) of oxygen tension within gels *in vivo*. Blood glucose and body weight evaluated by parametric unpaired t-test. Average area and percent islet area evaluated by two-way ANOVA with Sidak's multiple comparisons test. N = 5. Error = SEM, scale bars panel C = 500 µm, panel D = 100 µm. * $P < 0.05$. N.S. = no significance

Table 1

Parameters for *in vitro* COMSOL model of oxygen profile within gels.

Parameter	Value	Property
R_{oxy}	-2.5×10^{-4} mol/(m^3*s)	Rate of oxygen consumption within gel
C_{oxy0}	0.2 mol/m^3	Initial oxygen concentration in gel
$C_{oxy\ boundary}$	0.2 mol/m^3	Oxygen concentration at gel border
D_{oxy}	2.7×10^{-9} m^2/s	Diffusion coefficient of oxygen within hydrogels

Table 2

Parameters for *in vivo* COMSOL model of oxygen profile within gels.

Parameter	Value	Property
R_{oxy}	-2.5×10^{-4} mol/(m^3*s)	Rate of oxygen consumption by islets within gel
C_{oxy0}	0.2 mol/m^3	Initial oxygen concentration in gel
$C_{oxy\ boundaryVEGF}$	0.0723 mol/m^3	Oxygen concentration at gel border for VEGF condition
$C_{oxy\ boundaryCtrl}$	0.0639 mol/m^3	Oxygen concentration at gel border for Control condition
D_{oxy}	2.7×10^{-9} m^2/s	Diffusion coefficient of oxygen within hydrogels